Transport Measurements of Majorization Order for Wave Coherence

Cheng Guo,* David A. B. Miller, and Shanhui Fan†
Ginzton Laboratory and Department of Electrical Engineering, Stanford University, Stanford, California 94305, USA

(Received 10 August 2024; revised 17 April 2025; accepted 26 June 2025; published 30 July 2025)

We investigate the majorization order for comparing wave coherence and reveal its fundamental consequences in transport measurements, including power distribution, absorption, transmission, and reflection. We prove that all these measurements preserve the majorization order under unitary control, enabling direct experimental characterization of the majorization order. Specifically, waves with lower coherence in the majorization order exhibit more restricted ranges of achievable measurement values. Our results deepen the understanding of coherence in transport phenomena.

DOI: 10.1103/snx3-bbx1

Wave coherence originates from the statistical properties of random fluctuations [1–4] and plays a crucial role in fundamental phenomena like interference, diffraction, and scattering [5–8]. Coherence theory examines how coherence affects observables [9]. A fundamental issue in coherence theory is the comparison of coherence between different waves. The concept of "degree of coherence" can be formalized through various measures, each with specific applications and limitations. For instance, von Laue's entropy measure [10,11] has clear thermodynamic significance but is coarse due to its scalar nature [6]. Other measures addressing different aspects of coherence were proposed by Zernike [12], Glauber [5], Mandel and Wolf [3], among others [7,13–18].

Quantum resource theories have advanced coherence theory [19–23], introducing a new coherence measure based on the majorization order [24–28]. This measure offers clear algebraic and geometric interpretations, and computational simplicity [29]. However, its unique physical implications, especially for classical waves, remain unclear. Certainly, any coherence measure, including majorization order, can be indirectly inferred from density matrix tomography [30–32]. However, direct measurements specific to the majorization order effects are yet to be established.

In this Letter, we reveal the fundamental consequences of the majorization order in transport measurements, including power distribution, absorption, transmission, and reflection. We demonstrate that these measurements, under unitary control (i.e., unitary transformations of the input wave), precisely preserve and manifest the majorization order, distinguishing it from other coherence measures. Consequently, these effects enable direct experimental characterization of the majorization order. Our findings highlight the crucial role of the majorization order in transport phenomena and coherence theory.

We begin by reviewing the density matrix formalism of wave coherence. We consider an n-dimensional Hilbert space of waves [33] and focus on the second-order coherence phenomena [7,9]. In this formalism, a wave is represented by a density matrix $\rho \in M_n$ [4,8,11,34–40], also known as a coherence [41] or coherency [2,42,43] matrix in optics. Here, M_n denotes the set of $n \times n$ complex matrices. The density matrix ρ is Hermitian and positive semidefinite. A normalized density matrix satisfies

$$\mathrm{tr}\rho = 1. \tag{1}$$

The coherence properties of the wave are encoded in the eigenvalues of ρ, which we call the coherence spectrum:

$$\boldsymbol{\lambda}^{\downarrow}(\rho) = (\lambda_1^{\downarrow}(\rho), \ldots, \lambda_n^{\downarrow}(\rho)), \tag{2}$$

where $\downarrow$ denotes reordering the components in nonincreasing order, which is in principle directly measurable [30–32]. A perfectly coherent wave has $\boldsymbol{\lambda}^{\downarrow}(\rho) = (1, 0, \ldots, 0)$, while a fully incoherent wave has $\boldsymbol{\lambda}^{\downarrow}(\rho) = (1/n, 1/n, \ldots, 1/n)$. For any wave, $\boldsymbol{\lambda}^{\downarrow}(\rho)$ belongs to the set of ordered n-dimensional probability vectors:

$$\Delta_n^{\downarrow} = \left\{ \boldsymbol{x} \in \mathbb{R}^n | x_i \geq 0, x_i \geq x_{i+1}, \sum_{i=1}^{n} x_i = 1 \right\}. \tag{3}$$

To compare the coherence of waves, one must introduce an order on $\Delta_n^{\downarrow}$. One approach is to use the entropy

$$H(\rho) = -\sum_{i=1}^{n} \lambda_i^{\downarrow}(\rho) \ln \lambda_i^{\downarrow}(\rho), \tag{4}$$

and define ρ_1 to be less coherent than ρ_2 in the entropy order if $H(\rho_1) > H(\rho_2)$ [10,11]. We focus on an alternative order based on majorization. For vectors $\boldsymbol{x}$ and $\boldsymbol{y}$ in $\mathbb{R}^n$, $\boldsymbol{x}$ is

*Contact author: guocheng@stanford.edu
†Contact author: shanhui@stanford.edu

majorized by $\boldsymbol{y}$, denoted as $\boldsymbol{x} \prec \boldsymbol{y}$ [29], if

$$\sum_{i=1}^{k} x_i^{\downarrow} \le \sum_{i=1}^{k} y_i^{\downarrow}, \quad \text{for all } k = 1, 2, \ldots, n-1; \tag{5}$$

$$\sum_{i=1}^{n} x_i = \sum_{i=1}^{n} y_i. \tag{6}$$

Intuitively, $\boldsymbol{x} \prec \boldsymbol{y}$ means that the components of $\boldsymbol{x}$ are no more spread out than those of $\boldsymbol{y}$. The set $\Delta_n^{\downarrow}$, together with the majorization relation, denoted as $\langle \Delta_n^{\downarrow}, \prec \rangle$, forms a partially ordered set, thus $\prec$ is reflexive, antisymmetric, and transitive on $\Delta_n^{\downarrow}$ [29]. For vectors $\boldsymbol{x}$ and $\boldsymbol{y}$ in $\Delta_n^{\downarrow}$, if $\boldsymbol{x} \prec \boldsymbol{y}$ and $\boldsymbol{x} \neq \boldsymbol{y}$, then $\boldsymbol{x}$ is strictly majorized by $\boldsymbol{y}$, denoted as $\boldsymbol{x} \precneqq \boldsymbol{y}$. If neither $\boldsymbol{x} \prec \boldsymbol{y}$ nor $\boldsymbol{y} \prec \boldsymbol{x}$ holds, then $\boldsymbol{x}$ and $\boldsymbol{y}$ are incomparable, denoted as $\boldsymbol{x} \| \boldsymbol{y}$ [44]. Incomparability can occur when $n \ge 3$. [See Supplemental Material (SM) [45], Secs. VI and VII for more details.] Comparing ρ_1 and ρ_2 using the majorization order, we obtain four possibilities: (1) $\boldsymbol{\lambda}^{\downarrow}(\rho_1) = \boldsymbol{\lambda}^{\downarrow}(\rho_2)$: they have the same coherence. (2) $\boldsymbol{\lambda}^{\downarrow}(\rho_1) \precneqq \boldsymbol{\lambda}^{\downarrow}(\rho_2)$: ρ_1 is less coherent than ρ_2. (3) $\boldsymbol{\lambda}^{\downarrow}(\rho_2) \precneqq \boldsymbol{\lambda}^{\downarrow}(\rho_1)$: ρ_1 is more coherent than ρ_2. (4) $\boldsymbol{\lambda}^{\downarrow}(\rho_1) \| \boldsymbol{\lambda}^{\downarrow}(\rho_2)$: their coherence is incomparable. As a sanity check, for any partially coherent wave ρ,

$$\left(\frac{1}{n}, \frac{1}{n}, \ldots, \frac{1}{n}\right) \precneqq \boldsymbol{\lambda}^{\downarrow}(\rho) \precneqq (1, 0, \ldots, 0). \tag{7}$$

Incomparable cases are typical rather than exceptional. It has been proved that the probability that two independent random vectors $\boldsymbol{\lambda}^{\downarrow}(\rho_1)$ and $\boldsymbol{\lambda}^{\downarrow}(\rho_2)$ uniformly distributed in $\Delta_n^{\downarrow}$ are comparable approaches zero as $n \to \infty$ (scaling asymptotically as $0.98n^{-0.41}$) [51,52].

The majorization order provides a different comparison from the entropy order. It can be shown that [29,53]

$$\boldsymbol{\lambda}^{\downarrow}(\rho_1) \precneqq \boldsymbol{\lambda}^{\downarrow}(\rho_2) \Longrightarrow H(\rho_1) > H(\rho_2). \tag{8}$$

However, the converse is not necessarily true. In fact,

$$H(\rho_1) > H(\rho_2) \Longrightarrow \boldsymbol{\lambda}^{\downarrow}(\rho_1) \precneqq \boldsymbol{\lambda}^{\downarrow}(\rho_2) \quad \text{or} \quad \boldsymbol{\lambda}^{\downarrow}(\rho_1) \| \boldsymbol{\lambda}^{\downarrow}(\rho_2). \tag{9}$$

Moreover, recent experiments have confirmed the existence of partially coherent optical waves that possess identical entropy values yet remain incomparable in the majorization order [54].

As examples that will be often used later, consider five 3×3 density matrices ρ_a to ρ_e with

$$\begin{aligned} &\boldsymbol{\lambda}^{\downarrow}(\rho_a) = (0.33, 0.33, 0.33), \quad \boldsymbol{\lambda}^{\downarrow}(\rho_b) = (0.60, 0.30, 0.10), \\ &\boldsymbol{\lambda}^{\downarrow}(\rho_c) = (0.80, 0.15, 0.05), \quad \boldsymbol{\lambda}^{\downarrow}(\rho_d) = (1.00, 0.00, 0.00), \\ &\boldsymbol{\lambda}^{\downarrow}(\rho_e) = (0.55, 0.45, 0.00). \end{aligned} \tag{10}$$

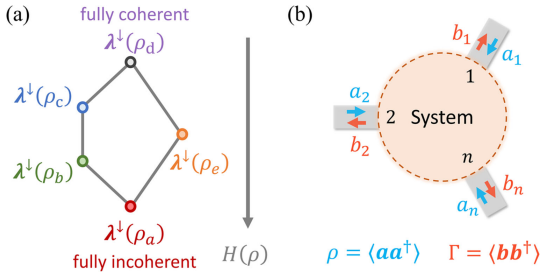

FIG. 1. (a) Hasse diagram for $\boldsymbol{\lambda}^{\downarrow}(\rho_a)$ to $\boldsymbol{\lambda}^{\downarrow}(\rho_e)$. An edge indicates a strict majorization relation between the lower and upper vertices. A higher vertical position indicates a lower entropy $H(\rho)$. (b) An n-port linear time-invariant system.

The majorization order indicates that

$$\boldsymbol{\lambda}^{\downarrow}(\rho_a) \precneqq \boldsymbol{\lambda}^{\downarrow}(\rho_b) \precneqq \boldsymbol{\lambda}^{\downarrow}(\rho_c) \precneqq \boldsymbol{\lambda}^{\downarrow}(\rho_d), \tag{11}$$

$$\boldsymbol{\lambda}^{\downarrow}(\rho_a) \precneqq \boldsymbol{\lambda}^{\downarrow}(\rho_e) \precneqq \boldsymbol{\lambda}^{\downarrow}(\rho_d), \tag{12}$$

$$\boldsymbol{\lambda}^{\downarrow}(\rho_b) \| \boldsymbol{\lambda}^{\downarrow}(\rho_e), \quad \boldsymbol{\lambda}^{\downarrow}(\rho_c) \| \boldsymbol{\lambda}^{\downarrow}(\rho_e). \tag{13}$$

In contrast, the entropy order indicates that

$$H(\rho_a) > H(\rho_b) > H(\rho_e) > H(\rho_c) > H(\rho_d). \tag{14}$$

These relations are summarized in a Hasse diagram [44] [Fig. 1(a)], where the edges indicate the majorization order and the height indicates the entropy order.

This Letter aims to demonstrate the fundamental role of the majorization order in transport processes. Resource theories treat coherence as a resource that constrains achievable observables [19,21]. This perspective motivates us to examine the range of achievable transport responses for input waves with a specific coherence spectrum $\boldsymbol{\lambda}^{\downarrow}(\rho)$. We will show that waves with lower coherence in the majorization order exhibit more constrained ranges of achievable outcomes in transport processes.

Specifically, we consider a linear system where an input wave ρ yields a response $F(\rho)$, with F representing power distribution, absorption, transmission, or reflection. We generate all waves with identical total power and coherence spectrum as ρ via unitary control, which transforms the input wave according to

$$\rho \to \rho[U] = U\rho U^{\dagger}. \tag{15}$$

We examine the set of all achievable responses:

$$\{F\} \coloneqq \{F(\rho[U]) | U \in U(n)\}. \tag{16}$$

We show that this set preserves the majorization order: for sets $\{F\}_1$ and $\{F\}_2$ corresponding to waves ρ_1 and ρ_2, respectively,

$$\boldsymbol{\lambda}^{\downarrow}(\rho_1) \prec \boldsymbol{\lambda}^{\downarrow}(\rho_2) \Longrightarrow \{F\}_1 \subseteq \{F\}_2. \tag{17}$$

This result reveals the direct physical consequences of the majorization order. Moreover, the converse of Eq. (17) often holds. Thus, measuring $\{F\}$ enables experimental comparison of coherence in the majorization order.

We begin our detailed analysis by reviewing the scattering matrix and unitary control. Consider an n-port linear time-invariant system characterized by a scattering matrix $S \in M_n$ [55] [Fig. 1(b)]. A coherent input wave, represented by vector $\boldsymbol{a}$, scatters into an output wave $\boldsymbol{b} = S\boldsymbol{a}$. A partially coherent input wave is described by a density matrix:

$$\rho = \langle \boldsymbol{a}\boldsymbol{a}^\dagger \rangle, \tag{18}$$

where $\langle\cdot\rangle$ denotes the average over an ensemble of realizations of randomly fluctuating fields [9]. The diagonal elements of ρ, denoted by $\boldsymbol{d}(\rho)$, specify the input power in each port, while $\mathrm{tr}\rho$ gives the total input power, assumed to be unity [Eq. (1)]. The output wave is characterized by an unnormalized density matrix:

$$\Gamma = \langle \boldsymbol{b}\boldsymbol{b}^\dagger \rangle = S\rho S^\dagger. \tag{19}$$

The diagonal elements of Γ represent the output power in each port, and $\mathrm{tr}\Gamma$ is the total output power, which may differ from unity in systems with loss or gain.

For a lossless system, the scattering matrix is unitary, denoted as U. The output density matrix then becomes $\rho[U]$ as defined in Eq. (15). This process is called unitary control of the density matrix. Unitary control preserves both the total power and the coherence spectrum:

$$\mathrm{tr}\rho[U] = 1, \qquad \boldsymbol{\lambda}^{\downarrow}(\rho[U]) = \boldsymbol{\lambda}^{\downarrow}(\rho). \tag{20}$$

Conversely, any pair of waves with identical total power and coherence spectrum can be interconverted through unitary control. Therefore, the set

$$\{\rho[U] | U \in U(n)\} \tag{21}$$

comprises all waves with the same total power and coherence spectrum as ρ.

Unitary control can be implemented using programmable unitary converters such as spatial light modulators [56–58], Mach-Zehnder interferometers [59–72], and multiplane light conversion devices [73–78]. It has been introduced to manipulate the absorption, transmission, and reflection of both coherent [79–81] and partially coherent waves [46,82]. Here, we examine four transport measurements under unitary control: power distribution, absorption, transmission, and reflection.

First, we consider the power distribution measurement [Fig. 2(a)]. We apply unitary control [Eq. (15)] to an input wave ρ and measure the power distribution in each port:

$$\boldsymbol{d}(\rho[U]) = \boldsymbol{d}(U\rho U^\dagger), \tag{22}$$

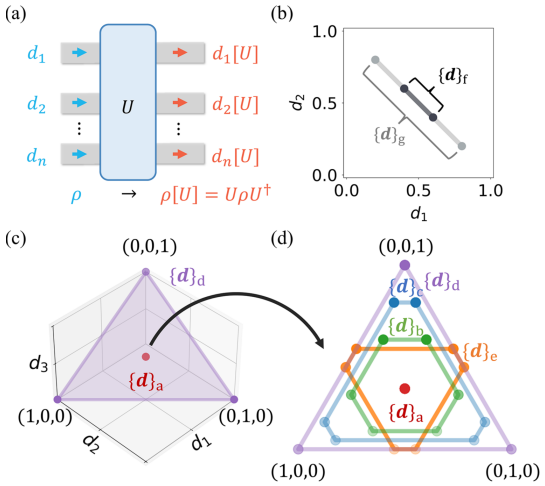

FIG. 2. (a) Scheme of unitary control. The power distribution $\boldsymbol{d}(\rho) \to \boldsymbol{d}(U\rho U^\dagger)$. (b) $\{\boldsymbol{d}\}$ for ρ_f and ρ_g. (c),(d) $\{\boldsymbol{d}\}$ for ρ_a to ρ_e. (c) A 3D plot. All $\{\boldsymbol{d}\}$ lie in the plane $d_1 + d_2 + d_3 = 1$. (d) Each set $\{\boldsymbol{d}\}$ in the plane. Only the boundaries are shown.

which corresponds to the vector of the diagonal elements of $\rho[U]$. It can be shown that the set of all achievable power distribution vectors under unitary control is

$$\begin{aligned}\{\boldsymbol{d}\} &:= \{\boldsymbol{d}(\rho[U]) | U \in U(n)\} \\ &= \{\boldsymbol{u} \in \mathbb{R}^n | \boldsymbol{u} \prec \boldsymbol{\lambda}^{\downarrow}(\rho)\}.\end{aligned} \tag{23}$$

See SM, Sec. I [45] for proof of Eq. (23) using the Schur-Horn theorem [29,83]. Equation (23) has a simple geometric interpretation: $\{\boldsymbol{d}\}$ is the convex hull spanned by the $n!$ points obtained by permuting the coordinates of $\boldsymbol{\lambda}^{\downarrow}(\rho)$. See Figs. 2(b) and 2(d) for examples of $\{\boldsymbol{d}\}$ when $n = 2$ and 3, respectively.

Next, consider two input waves ρ_1 and ρ_2 with their corresponding sets $\{\boldsymbol{d}\}_1$ and $\{\boldsymbol{d}\}_2$. One can prove that

$$\boldsymbol{\lambda}^{\downarrow}(\rho_1) \prec \boldsymbol{\lambda}^{\downarrow}(\rho_2) \Longleftrightarrow \{\boldsymbol{d}\}_1 \subseteq \{\boldsymbol{d}\}_2. \tag{24}$$

More precisely, considering all four possibilities:

$$\boldsymbol{\lambda}^{\downarrow}(\rho_1) = \boldsymbol{\lambda}^{\downarrow}(\rho_2) \Longleftrightarrow \{\boldsymbol{d}\}_1 = \{\boldsymbol{d}\}_2, \tag{25}$$

$$\boldsymbol{\lambda}^{\downarrow}(\rho_1) \precneqq \boldsymbol{\lambda}^{\downarrow}(\rho_2) \Longleftrightarrow \{\boldsymbol{d}\}_1 \subsetneq \{\boldsymbol{d}\}_2, \tag{26}$$

$$\boldsymbol{\lambda}^{\downarrow}(\rho_2) \precneqq \boldsymbol{\lambda}^{\downarrow}(\rho_1) \Longleftrightarrow \{\boldsymbol{d}\}_2 \subsetneq \{\boldsymbol{d}\}_1, \tag{27}$$

$$\boldsymbol{\lambda}^{\downarrow}(\rho_1) \parallel \boldsymbol{\lambda}^{\downarrow}(\rho_2) \Longleftrightarrow \{\boldsymbol{d}\}_1 \parallel \{\boldsymbol{d}\}_2. \tag{28}$$

Here, $A \parallel B$ for two sets A and B means that they partially overlap, i.e., they intersect, but neither is a subset of the other. See SM, Sec. II [45] for detailed proofs of Eqs. (24)–(28). Therefore, the power distribution measurement exactly preserves the majorization order and offers an experimental method to probe the majorization order.

We provide two illustrative examples. The first example concerns two 2×2 density matrices ρ_f and ρ_g with

$$\boldsymbol{\lambda}^{\downarrow}(\rho_f) = (0.60, 0.40), \qquad \boldsymbol{\lambda}^{\downarrow}(\rho_g) = (0.80, 0.20). \tag{29}$$

Figure 2(b) depicts the sets $\{\boldsymbol{d}\}_f$ and $\{\boldsymbol{d}\}_g$ as given by Eq. (23). These sets are line segments with end points obtained by permuting the coordinates of $\boldsymbol{\lambda}^{\downarrow}(\rho_f)$ and $\boldsymbol{\lambda}^{\downarrow}(\rho_g)$, respectively. We note that $\{\boldsymbol{d}\}_f \subsetneqq \{\boldsymbol{d}\}_g$ because $\boldsymbol{\lambda}^{\downarrow}(\rho_f) \precneqq \boldsymbol{\lambda}^{\downarrow}(\rho_g)$.

The second example concerns the five 3×3 density matrices ρ_a to ρ_e introduced in Eq. (10). Figures 2(c) and 2(d) depict the sets $\{\boldsymbol{d}\}_a$ to $\{\boldsymbol{d}\}_e$ as given by Eq. (23). These sets are convex hexagons with vertices obtained by permuting the coordinates of $\boldsymbol{\lambda}^{\downarrow}(\rho_a)$ to $\boldsymbol{\lambda}^{\downarrow}(\rho_e)$, respectively. ($\{\boldsymbol{d}\}_a$ and $\{\boldsymbol{d}\}_d$ are degenerate hexagons with coalescing vertices.) We note that

$$\{\boldsymbol{d}\}_a \subsetneqq \{\boldsymbol{d}\}_b \subsetneqq \{\boldsymbol{d}\}_c \subsetneqq \{\boldsymbol{d}\}_d, \tag{30}$$

$$\{\boldsymbol{d}\}_a \subsetneqq \{\boldsymbol{d}\}_e \subsetneqq \{\boldsymbol{d}\}_d, \tag{31}$$

$$\{\boldsymbol{d}\}_b \parallel \{\boldsymbol{d}\}_e, \qquad \{\boldsymbol{d}\}_c \parallel \{\boldsymbol{d}\}_e, \tag{32}$$

which confirm Eqs. (25)–(28) applied to Eqs. (11)–(13).

Second, we consider the absorption measurement [Fig. 3(a)]. We input a wave ρ into a system with a scattering matrix S and measure the total absorption:

$$\alpha[S] = \mathrm{tr}(\rho A), \tag{33}$$

where A is the absorptivity matrix [79,84], defined as

$$A \coloneqq I - S^{\dagger}S. \tag{34}$$

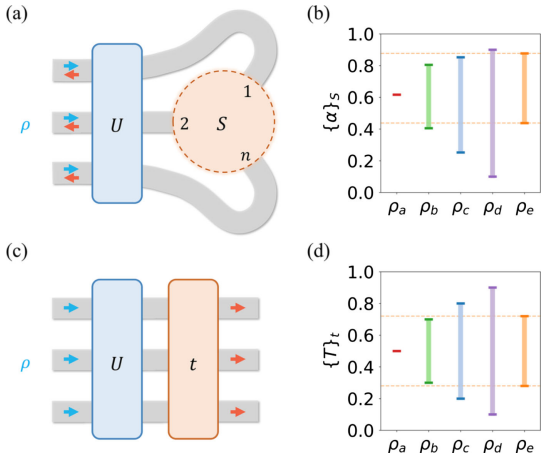

FIG. 3. (a) Total absorption measurement with unitary control. (b) $\{\alpha\}_S$ for ρ_a to ρ_e where $\boldsymbol{\sigma}^{\downarrow}(S) = (0.95, 0.39, 0.32)$. (c) Total transmission measurement with unitary control. (d) $\{T\}_t$ for ρ_a to ρ_e where $\boldsymbol{\sigma}^{\downarrow}(t) = (0.95, 0.71, 0.32)$.

We apply unitary control [Eq. (15)] to transform the input wave ρ. The total absorption then changes to

$$\alpha[S] \to \alpha[S, U] = \mathrm{tr}(U\rho U^{\dagger}A). \tag{35}$$

It has been shown that the set of all achievable total absorption values under unitary control is [46]

$$\begin{aligned}\{\alpha\}_S &\coloneqq \{\alpha[S, U] | U \in U(n)\} \\ &= [\boldsymbol{\lambda}^{\downarrow}(\rho) \cdot \boldsymbol{\lambda}^{\uparrow}(A), \boldsymbol{\lambda}^{\downarrow}(\rho) \cdot \boldsymbol{\lambda}^{\downarrow}(A)]\end{aligned} \tag{36}$$

with the absorption eigenvalues given by [85]

$$\boldsymbol{\lambda}^{\downarrow}(A) = \mathbf{1} - \boldsymbol{\sigma}^{2\uparrow}(S) = (1 - \sigma_1^{2\uparrow}, \ldots, 1 - \sigma_n^{2\uparrow}), \tag{37}$$

where $\boldsymbol{\sigma}(S)$ denotes the vector of singular values of S, $\uparrow$ indicates reordering the components in nondecreasing order, $[,]$ denotes the close real interval, and $\cdot$ represents the usual inner product. See SM, Sec. III [45] for an intuitive interpretation of Eq. (36).

Next, consider two waves ρ_1 and ρ_2 with their corresponding sets $\{\alpha\}_{S,1}$ and $\{\alpha\}_{S,2}$. One can prove that [46]

$$\boldsymbol{\lambda}^{\downarrow}(\rho_1) \prec \boldsymbol{\lambda}^{\downarrow}(\rho_2) \Longleftrightarrow \forall\, S \in M_n, \{\alpha\}_{S,1} \subseteq \{\alpha\}_{S,2}. \tag{38}$$

Thus, the total absorption measurement preserves the majorization order. More precisely,

$$\boldsymbol{\lambda}^{\downarrow}(\rho_1) = \boldsymbol{\lambda}^{\downarrow}(\rho_2) \Longleftrightarrow \forall\, S \in M_n, \{\alpha\}_{S,1} = \{\alpha\}_{S,2}; \tag{39}$$

$$\begin{aligned}\boldsymbol{\lambda}^{\downarrow}(\rho_1) \precneqq \boldsymbol{\lambda}^{\downarrow}(\rho_2) \Longleftrightarrow \forall\, S \in M_n, \{\alpha\}_{S,1} \subseteq \{\alpha\}_{S,2} \quad &\text{and} \\ \exists\, \tilde{S} \in M_n, \{\alpha\}_{\tilde{S},1} \neq \{\alpha\}_{\tilde{S},2}; \quad &\end{aligned} \tag{40}$$

$$\begin{aligned}\boldsymbol{\lambda}^{\downarrow}(\rho_2) \precneqq \boldsymbol{\lambda}^{\downarrow}(\rho_1) \Longleftrightarrow \forall\, S \in M_n, \{\alpha\}_{S,2} \subseteq \{\alpha\}_{S,1} \quad &\text{and} \\ \exists\, \tilde{S} \in M_n, \{\alpha\}_{\tilde{S},2} \neq \{\alpha\}_{\tilde{S},1}; \quad &\end{aligned} \tag{41}$$

$$\begin{aligned}\boldsymbol{\lambda}^{\downarrow}(\rho_1) \parallel \boldsymbol{\lambda}^{\downarrow}(\rho_2) \Longleftrightarrow \exists\, S \in M_n, \{\alpha\}_{S,1} \nsubseteq \{\alpha\}_{S,2} \quad &\text{and} \\ \exists\, \tilde{S} \in M_n, \{\alpha\}_{\tilde{S},2} \nsubseteq \{\alpha\}_{\tilde{S},1}. \quad &\end{aligned} \tag{42}$$

See SM, Sec. IV [45] for detailed proofs of Eqs. (38)–(42). We highlight the similarities and differences between Eqs. (25)–(28) and (39)–(42). The differences reflect the fact that the absorption measurements also depend on the properties of the S matrix.

As an illustration, Fig. 3(b) depicts $\{\alpha\}_S$ as given by Eq. (36) for ρ_a to ρ_e and a 3×3 S matrix with $\boldsymbol{\sigma}^{\downarrow}(S) = (0.95, 0.39, 0.32)$. We note that

$$\{\alpha\}_{S,a} \subsetneqq \{\alpha\}_{S,b} \subsetneqq \{\alpha\}_{S,c} \subsetneqq \{\alpha\}_{S,d}, \tag{43}$$

$$\{\alpha\}_{S,a} \subsetneqq \{\alpha\}_{S,e} \subsetneqq \{\alpha\}_{S,d}, \tag{44}$$

$$\{\alpha\}_{S,b} \parallel \{\alpha\}_{S,e}, \quad \{\alpha\}_{S,c} \parallel \{\alpha\}_{S,e}, \tag{45}$$

which confirm Eqs. (39)–(42) applied to Eqs. (11)–(13).

The total absorption measurement can also probe the majorization order. We consider two experimental settings. In the first setting, we have a single lossy system with an unknown scattering matrix S. We perform total absorption measurements under unitary control and obtain $\{\alpha\}_{S,1}$ and $\{\alpha\}_{S,2}$. By comparing $\{\alpha\}_{S,1}$ and $\{\alpha\}_{S,2}$, we can infer the relation between $\boldsymbol{\lambda}^{\downarrow}(\rho_1)$ and $\boldsymbol{\lambda}^{\downarrow}(\rho_2)$ [86]:

$$\{\alpha\}_{S,1} = \{\alpha\}_{S,2} \Longrightarrow \text{no information}; \tag{46}$$

$$\{\alpha\}_{S,1} \subsetneqq \{\alpha\}_{S,2} \Longrightarrow \boldsymbol{\lambda}^{\downarrow}(\rho_1) \precneqq \boldsymbol{\lambda}^{\downarrow}(\rho_2) \quad \text{or} \quad \boldsymbol{\lambda}^{\downarrow}(\rho_1) \parallel \boldsymbol{\lambda}^{\downarrow}(\rho_2); \tag{47}$$

$$\{\alpha\}_{S,2} \subsetneqq \{\alpha\}_{S,1} \Longrightarrow \boldsymbol{\lambda}^{\downarrow}(\rho_2) \precneqq \boldsymbol{\lambda}^{\downarrow}(\rho_1) \quad \text{or} \quad \boldsymbol{\lambda}^{\downarrow}(\rho_1) \parallel \boldsymbol{\lambda}^{\downarrow}(\rho_2); \tag{48}$$

$$\{\alpha\}_{S,1} \parallel \{\alpha\}_{S,2} \Longrightarrow \boldsymbol{\lambda}^{\downarrow}(\rho_1) \parallel \boldsymbol{\lambda}^{\downarrow}(\rho_2). \tag{49}$$

See SM, Sec. V [45] for detailed proofs of Eqs. (46)–(49). Only the last case yields a definite relation [Eq. (49)].

Equations (46)–(49) demonstrate that a single lossy system may not provide sufficient information to definitively determine the relation between arbitrary $\boldsymbol{\lambda}^{\downarrow}(\rho_1)$ and $\boldsymbol{\lambda}^{\downarrow}(\rho_2)$. To address this limitation, we perform absorption measurements on a set of lossy systems with designed scattering matrices. The minimum number of systems required is $\lceil (n-1)/2 \rceil$, where $\lceil \cdot \rceil$ represents the ceiling function. This number is necessary because comparing $\{\alpha\}_{S,1}$ and $\{\alpha\}_{S,2}$ in one system produces two inequalities, while verifying the majorization order requires $(n-1)$ inequalities [Eq. (5)]. To show that this number is also sufficient, consider the following set of systems:

$$S_m = \begin{pmatrix} I_{n-m} & O \\ O & O \end{pmatrix}, \qquad m = 1, 2, \ldots, \lceil \frac{n-1}{2} \rceil. \tag{50}$$

Comparing $\{\alpha\}_{S_m,1}$ and $\{\alpha\}_{S_m,2}$ enables verification of all $(n-1)$ linear inequalities required for majorization, thus providing sufficient information to determine the definitive relation between any $\boldsymbol{\lambda}^{\downarrow}(\rho_1)$ and $\boldsymbol{\lambda}^{\downarrow}(\rho_2)$. This discussion motivates the following open question: How to decide whether an arbitrary set of systems S_j, $j = 1, 2, \ldots, k$, where $k \geq \lceil (n-1)/2 \rceil$, can provide sufficient information to definitely determine the majorization order?

Third, we consider the total transmission measurement [Fig. 3(c)]. We examine a system with a $2n \times 2n$ scattering matrix

$$\tilde{S} = \begin{pmatrix} r & t' \\ t & r' \end{pmatrix}, \tag{51}$$

where r and t are the $n \times n$ reflection and transmission matrices for input from the left, and r' and t' are the corresponding matrices for input from the right. We input a wave ρ from the left and measure the total transmission:

$$T[t] = \mathrm{tr}(\rho t^{\dagger} t). \tag{52}$$

We apply unitary control [Eq. (15)] to transform the input wave ρ. The total transmission then changes to

$$T[t] \to T[t, U] = \mathrm{tr}(U \rho U^{\dagger} t^{\dagger} t). \tag{53}$$

It has been shown that the set of all achievable total transmission values under unitary control is [82]

$$\begin{aligned} \{T\}_t &:= \{T[t, U] | U \in U(n)\} \\ &= [\boldsymbol{\lambda}^{\downarrow}(\rho) \cdot \boldsymbol{\sigma}^{2\uparrow}(t), \boldsymbol{\lambda}^{\downarrow}(\rho) \cdot \boldsymbol{\sigma}^{2\downarrow}(t)]. \end{aligned} \tag{54}$$

See SM, Sec. III [45] for an intuitive interpretation of Eq. (54).

Next, consider two waves ρ_1 and ρ_2 with their corresponding sets $\{T\}_{t,1}$ and $\{T\}_{t,2}$. One can prove that [82]

$$\boldsymbol{\lambda}^{\downarrow}(\rho_1) \prec \boldsymbol{\lambda}^{\downarrow}(\rho_2) \Longleftrightarrow \forall\, t \in M_n,\ \{T\}_{t,1} \subseteq \{T\}_{t,2}. \tag{55}$$

The remaining discussion is analogous to that of absorption and is omitted. The analysis of reflection is similar. As an illustration, Fig. 3(d) depicts $\{T\}_t$ as given by Eq. (54) for ρ_a to ρ_e and a 3×3 t matrix with $\boldsymbol{\sigma}^{\downarrow}(t) = (0.95, 0.71, 0.32)$, where

$$\{T\}_{t,a} \subsetneqq \{T\}_{t,b} \subsetneqq \{T\}_{t,e} \subsetneqq \{T\}_{t,c} \subsetneqq \{T\}_{t,d}, \tag{56}$$

which confirms Eq. (55) applied to Eqs. (11)–(13).

We make five final remarks. First, our findings apply to both classical and quantum waves, including optical, acoustic, and electronic varieties. Second, many of our results, especially those concerning incomparable cases, are not captured by other measures such as entropy order. Third, while we primarily compared coherence between wave pairs, this can be extended to multiple waves. The mathematical property that $\langle \Delta_n^{\downarrow}, \prec \rangle$ forms a complete lattice [44,47,48] ensures that any subset of waves has a well-defined supremum and infimum (see SM, Secs. VII and VIII [45]). Fourth, all discussed measurements require determining the range of responses under unitary control. It suffices to find the unitary transformations that achieve the extremal responses, which can be solved using efficient variational algorithms [87–92], without running over all unitary transformations in $U(n)$. Fifth, while we focus on transport measurements of classical waves (mixtures of coherent states), our majorization order results should extend to quantum waves with entanglement.

In conclusion, our investigation of the majorization order for comparing wave coherence has revealed its fundamental role in transport measurements. We have shown that these measurements preserve the majorization order under

unitary control, enabling direct experimental probes of this order for wave coherence. Our Letter provides a unifying framework for understanding coherence phenomena in wave transport, paving the way for improved coherence characterization and engineering in both classical and quantum technologies. Our theoretical proposal can be readily implemented in few-port systems using current wavefront shaping techniques [54]. Implementation in many-port systems would benefit from further advances in programmable unitary converters.

Acknowledgments—C. G. thanks Dr. Zhaoyou Wang for helpful discussions. This work is funded by a Simons Investigator in Physics grant from the Simons Foundation (Grant No. 827065) and by a Multidisciplinary University Research Initiative (MURI) grant from the U.S. Air Force Office of Scientific Research (AFOSR) (Grant No. FA9550-21-1-0312).

[1] M. Born and E. Wolf, *Principles of Optics: Electromagnetic Theory of Propagation, Interference and Diffraction of Light*, 7th ed. (Cambridge University Press, Cambridge; New York, 1999).
[2] J. W. Goodman, *Statistical Optics*, Wiley Classics Library (Wiley, New York, 2000).
[3] L. Mandel and E. Wolf, *Optical Coherence and Quantum Optics* (Cambridge University Press, Cambridge; New York, 1995).
[4] E. L. O'Neill, *Introduction to Statistical Optics* (Dover Publications, Mineola, NY, 2003), ISBN 978-0-486-43578-7.
[5] R. J. Glauber, The quantum theory of optical coherence, Phys. Rev. **130**, 2529 (1963).
[6] L. Mandel and E. Wolf, Coherence properties of optical fields, Rev. Mod. Phys. **37**, 231 (1965).
[7] J. Perina, *Coherence of Light*, 2nd ed. (D. Reidel Publishing Company, Dordrecht, Holland, 1985), ISBN 978-90-277-2004-7.
[8] O. Korotkova, *Theoretical Statistical Optics* (World Scientific, New Jersey; London; Singapore; Beijing; Shanghai; Hong Kong; Taipei; Chennai; Tokyo, 2022).
[9] E. Wolf, *Introduction to the Theory of Coherence and Polarization of Light* (Cambridge University Press, Cambridge, England, 2007).
[10] M. Laue, Die Entropie von partiell kohärenten Strahlenbündeln, Ann. Phys. (Berlin) **328**, 1 (1907).
[11] H. Gamo, Thermodynamic entropy of partially coherent light beams, J. Phys. Soc. Jpn. **19**, 1955 (1964).
[12] F. Zernike, The concept of degree of coherence and its application to optical problems, Physica (Amsterdam) **5**, 785 (1938).
[13] H. Gamo, Intensity matrix and degree of coherence, J. Opt. Soc. Am. **47**, 976 (1957).
[14] B. Karczewski, Degree of coherence of the electromagnetic field, Phys. Lett. **5**, 191 (1963).
[15] J. Tervo, T. Setälä, and A. T. Friberg, Degree of coherence for electromagnetic fields, Opt. Express **11**, 1137 (2003).
[16] P. Réfrégier and F. Goudail, Invariant degrees of coherence of partially polarized light, Opt. Express **13**, 6051 (2005).
[17] T. Setälä, J. Tervo, and A. T. Friberg, Contrasts of Stokes parameters in Young's interference experiment and electromagnetic degree of coherence, Opt. Lett. **31**, 2669 (2006).
[18] A. Luis, Degree of coherence for vectorial electromagnetic fields as the distance between correlation matrices, J. Opt. Soc. Am. A **24**, 1063 (2007).
[19] E. Chitambar and G. Gour, Quantum resource theories, Rev. Mod. Phys. **91**, 025001 (2019).
[20] G. Torun, O. Pusuluk, and Ö. E. Müstecaplioğlu, A compendious review of majorization-based resource theories: Quantum information and quantum thermodynamics, Turk. J. Phys. **47**, 141 (2023).
[21] A. Streltsov, G. Adesso, and M. B. Plenio, Colloquium: Quantum coherence as a resource, Rev. Mod. Phys. **89**, 041003 (2017).
[22] T. Baumgratz, M. Cramer, and M. B. Plenio, Quantifying coherence, Phys. Rev. Lett. **113**, 140401 (2014).
[23] A. Winter and D. Yang, Operational resource theory of coherence, Phys. Rev. Lett. **116**, 120404 (2016).
[24] M. A. Nielsen, Conditions for a class of entanglement transformations, Phys. Rev. Lett. **83**, 436 (1999).
[25] G. Gour, M. P. Müller, V. Narasimhachar, R. W. Spekkens, and N. Yunger Halpern, The resource theory of informational nonequilibrium in thermodynamics, Phys. Rep. **583**, 1 (2015).
[26] A. Luis, Coherence for vectorial waves and majorization, Opt. Lett. **41**, 5190 (2016).
[27] I. Bengtsson and K. Życzkowski, *Geometry of Quantum States: An Introduction to Quantum Entanglement*, 2nd ed. (Cambridge University Press, Cambridge, England, 2017).
[28] G. Gour, D. Jennings, F. Buscemi, R. Duan, and I. Marvian, Quantum majorization and a complete set of entropic conditions for quantum thermodynamics, Nat. Commun. **9**, 5352 (2018).
[29] A. W. Marshall, I. Olkin, and B. C. Arnold, *Inequalities: Theory of Majorization and Its Applications*, 2nd ed. (Springer Science+Business Media, LLC, New York, 2011).
[30] A. F. Abouraddy, K. H. Kagalwala, and B. E. A. Saleh, Two-point optical coherency matrix tomography, Opt. Lett. **39**, 2411 (2014).
[31] K. H. Kagalwala, H. E. Kondakci, A. F. Abouraddy, and B. E. A. Saleh, Optical coherency matrix tomography, Sci. Rep. **5**, 15333 (2015).
[32] C. Roques-Carmes, S. Fan, and D. Miller, Measuring, processing, and generating partially coherent light with self-configuring optics, arXiv:2402.00704.
[33] For example, n denotes the number of ports (or spatial modes) for a multiport system as shown in Fig. 1(b).
[34] D. Gabor, IV light and information, Prog. Opt. **1**, 109 (1961).
[35] E. C. G. Sudarshan, Equivalence of semiclassical and quantum mechanical descriptions of statistical light beams, Phys. Rev. Lett. **10**, 277 (1963).
[36] H. Gamo, III matrix treatment of partial coherence, in *Progress in Optics*, edited by E. Wolf (Elsevier, New York, 1964), Vol. 3, pp. 187–332.

[37] L. D. Landau and L. M. Lifshitz, *Quantum Mechanics: Non-Relativistic Theory*, 3rd ed. (Butterworth-Heinemann, Singapore, 1981).

[38] E. Wolf, Unified theory of coherence and polarization of random electromagnetic beams, Phys. Lett. A **312**, 263 (2003).

[39] B. de Lima Bernardo, Unified quantum density matrix description of coherence and polarization, Phys. Lett. A **381**, 2239 (2017).

[40] H. Zhang, C. W. Hsu, and O. D. Miller, Scattering concentration bounds: Brightness theorems for waves, Optica **6**, 1321 (2019).

[41] P.-E. Wolf and G. Maret, Weak localization and coherent backscattering of photons in disordered media, Phys. Rev. Lett. **55**, 2696 (1985).

[42] K. Yamazoe, Coherency matrix formulation for partially coherent imaging to evaluate the degree of coherence for image, J. Opt. Soc. Am. A **29**, 1529 (2012).

[43] C. Okoro, H. E. Kondakci, A. F. Abouraddy, and K. C. Toussaint, Demonstration of an optical-coherence converter, Optica **4**, 1052 (2017).

[44] B. A. Davey and H. A. Priestley, *Introduction to Lattices and Order*, 2nd ed. (Cambridge University Press, Cambridge, England, 2002).

[45] See Supplemental Material at http://link.aps.org/supplemental/10.1103/snx3-bbx1 for detailed proof of Eqs. (23)–(28), intuitive interpretations of Eqs. (36) and (54), detailed proof of Eqs. (38)–(42) and (46)–(49), ordered sets and lattices, majorization lattice, and majorization lattice for multiple waves, which includes Refs. [44,46–50].

[46] C. Guo and S. Fan, Unitary control of partially coherent waves. I. Absorption, Phys. Rev. B **110**, 035430 (2024).

[47] P. M. Alberti and A. Uhlmann, *Stochasticity and Partial Order: Doubly Stochastic Maps and Unitary Mixing*, Mathematics and Its Applications (D. Reidel Publishing Company, Dordrecht, Holland, 1982), ISBN 978-90-277-1350-6.

[48] R. B. Bapat, Majorization and singular values. III, Linear Algebra Appl. **145**, 59 (1991).

[49] G. M. Bosyk, G. Bellomo, F. Holik, H. Freytes, and G. Sergioli, Optimal common resource in majorization-based resource theories, New J. Phys. **21**, 083028 (2019).

[50] S. Roman, *Lattices and Ordered Sets*, 1st ed. (Springer, New York, NY, 2008).

[51] F. D. Cunden, P. Facchi, G. Florio, and G. Gramegna, Generic aspects of the resource theory of quantum coherence, Phys. Rev. A **103**, 022401 (2021).

[52] V. Jain, M. Kwan, and M. Michelen, Entangled states are typically incomparable, arXiv:2406.03335.

[53] F. Cicalese and U. Vaccaro, Supermodularity and subadditivity properties of the entropy on the majorization lattice, IEEE Trans. Inf. Theory **48**, 933 (2002).

[54] M. Harling, V. A. Kelkar, K. C. Toussaint, and A. F. Abouraddy, Isoentropic partially coherent optical fields that cannot be interconverted unitarily, Phys. Rev. A **110**, 013505 (2024).

[55] H. A. Haus, *Waves and Fields in Optoelectronics* (Prentice-Hall, Englewood Cliffs, NJ, 1984).

[56] I. M. Vellekoop and A. P. Mosk, Focusing coherent light through opaque strongly scattering media, Opt. Lett. **32**, 2309 (2007).

[57] S. M. Popoff, A. Goetschy, S. F. Liew, A. D. Stone, and H. Cao, Coherent control of total transmission of light through disordered media, Phys. Rev. Lett. **112**, 133903 (2014).

[58] H. Yu, K. Lee, and Y. Park, Ultrahigh enhancement of light focusing through disordered media controlled by mega-pixel modes, Opt. Express **25**, 8036 (2017).

[59] M. Reck, A. Zeilinger, H. J. Bernstein, and P. Bertani, Experimental realization of any discrete unitary operator, Phys. Rev. Lett. **73**, 58 (1994).

[60] D. A. B. Miller, Establishing optimal wave communication channels automatically, J. Lightwave Technol. **31**, 3987 (2013).

[61] D. A. B. Miller, Self-aligning universal beam coupler, Opt. Express **21**, 6360 (2013).

[62] D. A. B. Miller, Self-configuring universal linear optical component [Invited], Photonics Res. **1**, 1 (2013).

[63] J. Carolan, C. Harrold, C. Sparrow, E. Martín-López, N. J. Russell, J. W. Silverstone, P. J. Shadbolt, N. Matsuda, M. Oguma, M. Itoh, G. D. Marshall, M. G. Thompson, J. C. F. Matthews, T. Hashimoto, J. L. O'Brien, and A. Laing, Universal linear optics, Science **349**, 711 (2015).

[64] D. A. B. Miller, Perfect optics with imperfect components, Optica **2**, 747 (2015).

[65] W. R. Clements, P. C. Humphreys, B. J. Metcalf, W. S. Kolthammer, and I. A. Walmsley, Optimal design for universal multiport interferometers, Optica **3**, 1460 (2016).

[66] A. Ribeiro, A. Ruocco, L. Vanacker, and W. Bogaerts, Demonstration of a 4×4-port universal linear circuit, Optica **3**, 1348 (2016).

[67] C. M. Wilkes, X. Qiang, J. Wang, R. Santagati, S. Paesani, X. Zhou, D. a. B. Miller, G. D. Marshall, M. G. Thompson, and J. L. O'Brien, 60 dB high-extinction auto-configured Mach–Zehnder interferometer, Opt. Lett. **41**, 5318 (2016).

[68] A. Annoni, E. Guglielmi, M. Carminati, G. Ferrari, M. Sampietro, D. A. Miller, A. Melloni, and F. Morichetti, Unscrambling light—automatically undoing strong mixing between modes, Light Sci. Appl. **6**, e17110 (2017).

[69] D. A. B. Miller, Setting up meshes of interferometers—reversed local light interference method, Opt. Express **25**, 29233 (2017).

[70] D. Perez, I. Gasulla, F. J. Fraile, L. Crudgington, D. J. Thomson, A. Z. Khokhar, K. Li, W. Cao, G. Z. Mashanovich, and J. Capmany, Silicon photonics rectangular universal interferometer, Laser Photonics Rev. **11**, 1700219 (2017).

[71] N. C. Harris, J. Carolan, D. Bunandar, M. Prabhu, M. Hochberg, T. Baehr-Jones, M. L. Fanto, A. M. Smith, C. C. Tison, P. M. Alsing, and D. Englund, Linear programmable nanophotonic processors, Optica **5**, 1623 (2018).

[72] S. Pai, B. Bartlett, O. Solgaard, and D. A. B. Miller, Matrix optimization on universal unitary photonic devices, Phys. Rev. Appl. **11**, 064044 (2019).

[73] J.-F. Morizur, L. Nicholls, P. Jian, S. Armstrong, N. Treps, B. Hage, M. Hsu, W. Bowen, J. Janousek, and H.-A. Bachor, Programmable unitary spatial mode manipulation, J. Opt. Soc. Am. A **27**, 2524 (2010).

[74] G. Labroille, B. Denolle, P. Jian, P. Genevaux, N. Treps, and J.-F. Morizur, Efficient and mode selective spatial mode multiplexer based on multi-plane light conversion, Opt. Express **22**, 15599 (2014).

[75] R. Tanomura, Y. Taguchi, R. Tang, T. Tanemura, and Y. Nakano, Entropy of mode mixers for optical unitary converter based on multi-plane light conversion, in *Proceedings of the 2022 Conference on Lasers and Electro-Optics Pacific Rim* (Optica Publishing Group, 2022), p. CWP13A_02.

[76] H. Kupianskyi, S. A. R. Horsley, and D. B. Phillips, High-dimensional spatial mode sorting and optical circuit design using multi-plane light conversion, APL Photonics **8**, 026101 (2023).

[77] Y. Taguchi, Y. Wang, R. Tanomura, T. Tanemura, and Y. Ozeki, Iterative configuration of programmable unitary converter based on few-layer redundant multiplane light conversion, Phys. Rev. Appl. **19**, 054002 (2023).

[78] Y. Zhang and N. K. Fontaine, Multi-plane light conversion: A practical tutorial, arXiv:2304.11323.

[79] C. Guo and S. Fan, Majorization theory for unitary control of optical absorption and emission, Phys. Rev. Lett. **130**, 146202 (2023).

[80] C. Guo, D. A. B. Miller, and S. Fan, Unitary control of multiport wave transmission, Phys. Rev. A **111**, 023507 (2025).

[81] C. Guo and S. Fan, Topological winding guaranteed coherent orthogonal scattering, Phys. Rev. A **109**, L061503 (2024).

[82] C. Guo and S. Fan, Unitary control of partially coherent waves. II. Transmission or reflection, Phys. Rev. B **110**, 035431 (2024).

[83] H. Zhang, C. W. Hsu, and O. D. Miller, Scattering concentration bounds: Brightness theorems for waves, Optica **6**, 1321 (2019).

[84] D. A. B. Miller, L. Zhu, and S. Fan, Universal modal radiation laws for all thermal emitters, Proc. Natl. Acad. Sci. U.S.A. **114**, 4336 (2017).

[85] A. Yamilov, S. Petrenko, R. Sarma, and H. Cao, Shape dependence of transmission, reflection, and absorption eigenvalue densities in disordered waveguides with dissipation, Phys. Rev. B **93**, 100201(R) (2016).

[86] These are the only four possibilities since both $\{\alpha\}_{S,1}$ and $\{\alpha\}_{S,2}$ contain the point $(1/n)\sum_{i=1}^{n}[1-\sigma_i^2(S)]$.

[87] G. G. Guerreschi and M. Smelyanskiy, Practical optimization for hybrid quantum-classical algorithms, arXiv:1701.01450.

[88] K. Mitarai, M. Negoro, M. Kitagawa, and K. Fujii, Quantum circuit learning, Phys. Rev. A **98**, 032309 (2018).

[89] M. Schuld, V. Bergholm, C. Gogolin, J. Izaac, and N. Killoran, Evaluating analytic gradients on quantum hardware, Phys. Rev. A **99**, 032331 (2019).

[90] A. Mari, T. R. Bromley, and N. Killoran, Estimating the gradient and higher-order derivatives on quantum hardware, Phys. Rev. A **103**, 012405 (2021).

[91] M. Cerezo, A. Arrasmith, R. Babbush, S. C. Benjamin, S. Endo, K. Fujii, J. R. McClean, K. Mitarai, X. Yuan, L. Cincio, and P. J. Coles, Variational quantum algorithms, Nat. Rev. Phys. **3**, 625 (2021).

[92] V. Bergholm *et al.*, PennyLane: Automatic differentiation of hybrid quantum-classical computations, arXiv:1811.04968.